

Exposure Risk Assessment by Coupled Analysis of CFD and SIR model in Enclosed Space

Takayuki Fukuoka¹, Kazuhide Ito²,

¹ Graduate student, IGSES, Kyushu University, Fukuoka, Japan

² IGSES, Kyushu University, Fukuoka, Japan

Abstract

The indoor environment can play a significant role in the transmission and exposure of various contaminants. In some emerging aerial infections, such as influenza virus, tuberculosis virus, and other biological and chemical contaminants, the airborne route of transmission is thought to be important to evaluate exposure health risk. In this paper, first, we present the relationship between the classic SIR model proposed by Kermack & Mckendrick and the Wells-Riley model; then, we introduce the analytical procedure of coupled analysis of computational fluid dynamics (CFD)-based prediction of unsteady contaminant concentration distribution and the basic SIR model to predict exposure risk of residents in an enclosed space.

The classic SIR model consists of three differential equations coupling changes in the population of susceptibles (S), the population of infectors (I), and the population of recovery to an immune state (R). The Wells-Riley model can predict the number of susceptibles (S) as a function of infectious contaminant concentration and exposure time by respiration. Through the analysis of infectious contaminant concentration level in a large enclosure with CFD, prediction of the changes of S, I, and R becomes possible.

The results of sensitivity analysis with changes in ventilation rate and other parameters of infections for targeting a large enclosure with simple geometry showed non-uniform distribution of S, I, and R in enclosed spaces and indicated strong dependence on unsteady and inhomogeneous contaminant distribution.

Keywords: CFD, SIR, Infectious disease, Exposure risk

Introduction

The numbers of tuberculosis carriers and fatalities in Japan over recent years have been

extremely high among those of developed countries. Tuberculosis is an airborne infectious bioaerosol and its exposure risk is strongly affected by air flow conditions indoors. In 2009, the epidemic of influenza A (H1N1) became a serious issue and indoor air pollution problems caused by other airborne infectious bacteria, viruses, and pathogens were also recognized as social and public health concerns.

Concerning the exposure route between the generation source of infectious bioaerosols and residents, there are various pathways of transmission: transmission by direct contact, droplet contact, viral droplet nuclei transmission, fecal-oral transmission, oral transmission, and so on. In general, droplet contact and viral droplet nuclei transmission are called airborne route transmissions and the development of a prediction method for these transmission routes indoors is important with regard to the design of healthy indoor environments.

In this paper, first, we present the structure of fundamental epidemiological models, namely, the classic SIR model proposed by Kermack and Mckendrick and the Wells-Riley model; we also introduce the analytical procedure of coupled analysis of computational fluid dynamics (CFD)-based prediction of unsteady contaminant concentration distribution and the classic SIR model to predict exposure risk of residents in enclosed spaces. Generally, airborne infectious pathogens are transported by air movement indoors and coupled analysis of CFD and an epidemiological model is a significant predictive tool of health risk for indoor environmental design.

In this study, we focus on the coupled simulation of unsteady and non-uniform contaminant concentration distribution and infectious risk, which directly indicates the changes of population densities of susceptible, infectious, and recovered subjects in large enclosed spaces.

Outline of Epidemiological Model

The SIR model is a fundamental epidemiological model that represents propagation of transmission and was proposed by Kermack and McKendrick. The classic SIR model consists of three differential equations coupling the changes in the population of susceptibles (S), the population of infectors (I), and the population of recovery to an immune state (R). The basic equations of the SIR model are indicated in Table 1 (Equations (1) – (3)). The original SIR model defined by Kermack and McKendrick consists of only reaction term, and equations (1) – (3) constitute an extended model including the diffusion term. β is the contact rate between susceptibles and infectors [1/person/s], and γ is the recovery rate [1/s]. Basic reproductive ratio R_o is defined from β and γ as shown in equation (4), and has been used widely as a parameter that describes the average number of new cases that an infector produces in a particular population. $R_o > 1$ denotes that the infection rate is larger than the recovery or removal rate, which may lead to an epidemic and the spread of the infection. $R_o < 1$ indicates that the infection rate is smaller than the recovery rate, which may lead to an endemic

situation. Here, the equation $S+I+R=N (=S_0)$ is used.

On the other hand, a prediction model that quantitatively evaluates airborne infection risk was proposed by Wells in 1955 and modified by Riley et al. This model is known as the Wells-Riley equation as shown in equation (6) and it can predict the number of susceptibles (S) as a function of infectious contaminant concentration and exposure time by respiration. In equation (6), P_I is the probability of infection; C denotes the number of new cases of infectors; Q is the ventilation rate in a room [m^3/s]; q indicates the quanta production rate per infector [quanta/s]; p is the pulmonary ventilation rate of susceptibles [$\text{m}^3/\text{person}/\text{s}$]; and t is the duration of exposures [s]. Recently, numerical prediction results based on the Wells-Riley model in the case of a SARS outbreak in a hospital were reported by researchers in Hong Kong.

Here, the consistency between the traditional SIR model and the Wells-Riley equation is examined. Under the condition that (I) was much smaller than (S) and assumed to be constant, equation (1) in Table 1 became equation (7). Equation (7) became equation (8) for cases where $S_0=S+I$ and finally equation (9) was derived. Comparing the Wells-Riley equation shown in equation (6) and equation (9) derived from the SIR model, these equations were found to be analogous and equation (10) was introduced. Here, q/Q denotes the unit of concentration and β is a function of the concentration and pulmonary ventilation rate of susceptibles. The numerical prediction of the Wells-Riley model adopting the result of

unsteady and non-uniform concentration distribution estimated by CFD was essentially the same as the numerical prediction of the SIR model coupled with CFD analysis that took the early stage of infection spread into consideration.

Through the analysis of infectious contaminant concentration level and distribution in a large enclosure with CFD, the prediction of the number changes of (S), (I), and (R) becomes possible through the analysis of β .

Coupled Analysis of CFD and SIR Model in this Study

It was possible to predict unsteady and non-uniform concentration distribution by solving the scalar (aerial infectious contaminant) transport equation shown in equation (5) on the basis of flow field analysis by CFD. The time change of contact rate β distributions through unsteady concentration simulation in enclosed spaces and then equations (1)-(3) were solved using this time-dependent β . In the case that the infectors (I) emit infectious contaminant, namely, new contaminant sources, the source term S_ϕ that denotes the formation of scalar (new infectious contaminant) in equation (5) must be considered. In this study, S_ϕ and feedback from SIR analysis to scalar transport equation were disregarded.

The SIR model in Table 1 is an enhancing model that considers diffusion terms in (S), (I), and (R), and the movement of susceptibles or infectious could be reproduced approximately by giving the diffusion coefficient.

In particular, when the grid size of CFD is set to larger than human scale, the numerical results of diffusion and propagation of infectors become reasonable analyses that reproduce an actual phenomenon. In this case, SIR parameters indicate population density, that is, [population/m²].

In this study, unsteady and non-uniform concentration distribution was analyzed in three dimensions by CFD and governing equations of the SIR model were analyzed in two dimensions at a height of 1.6 m (y) from floor level (breathing zone level) as shown in Figure 1.

Outline of Sensitivity Analysis for Targeting Large Enclosed Spaces

Comparatively large enclosed spaces with a size of 10 m (x)×10 m (z)×3 m (y) and with a supply inlet opening with a size of 0.27 m×0.44 m near the floor and an exhaust outlet opening of the same size near the ceiling were assumed in this sensitivity analysis. The outline of the target enclosed space is shown in Figure 1. The infectious bioaerosols were assumed to be instantaneously generated in the center domain measuring 4 m (x) × 4 m (z) × 3 m (y) in the target enclosed space. The bioaerosols were assumed to be approximately passive contaminants and the unsteady and non-uniform distributions were analyzed during 24 hours with instantaneous generation. Flow fields were analyzed by the RNG k-ε model.

Table 2 denotes the numerical and boundary conditions of this sensitivity analysis. In this

sensitivity analysis, the population of infectors did not recover ($\gamma=0$) and they were assumed to die at a constant rate after infection. The γ in equation (9) was replaced with death rate (μ) in this analysis. The initial population of susceptibles S_0 was set at 100 and I_0 was assumed to be 10^{-2} . These values were not intended to reflect a specific or actual phenomenon. Ventilation rate (n) and pulmonary ventilation rate (p) were set to two levels and the contact rate (β) was calculated by pulmonary ventilation rate (p) and prediction results of contaminant concentration in the breathing zone. Death rate (μ) was set to ten times the contact rate (β).

CFD simulation is preferable to understand a non-uniform distribution in a comparatively short time scale. On the other hand, SIR-type epidemiology model is often used for infection transmission prediction for a long time scale, such as weeks or months. In this sensitivity analysis, the condition for highly infectious bioaerosols generated in the target space was assumed, and unsteady analyses were carried out for 24 hours. In accordance with the report by Fine (1993), the orders of basic reproductive ratio (R_o) were summarized as follows: $R_o=12-18$ for measles, $R_o=12-17$ for whooping cough (pertussis), $R_o=8-10$ for varicella, and $R_o=6-7$ for rubella. In this analysis, basic reproductive ratio (R_o) was set to 10 and other parameters including the contact rate (β) were determined appropriately.

Table 3 shows the cases analyzed. In Case 1 - Case 4, both susceptibles (S) and infectors (I) are assumed to remain stationary and do not move. In Case 5 - Case 8, both susceptibles (S)

and infectors (I) are assumed to move at a constant diffusion coefficient. In Case 9 - Case 12, it is assumed that only susceptibles (S) move by diffusion and infectors (I) remain stationary and do not move.

Results of Numerical Analysis

Figure 2 shows the results of flow field at $y=1.6$ m height for the case of a relatively low ventilation rate ($n=0.01 \text{ h}^{-1}$). This x - z plane does not contain supply and exhaust openings. A non-uniform distribution of flow field was confirmed and re-circulating flow was observed in the center of the analytical domain.

Figure 3 indicates the time series of contaminant concentration ϕ in the target space. The value of ϕ denotes the volume-averaged concentration for the whole space. In the case of a low ventilation rate ($n=0.01 \text{ h}^{-1}$), the nominal time constant was 100 h and the contaminant concentration ϕ was almost constant through the 24 h of analysis. In the case of a relatively high ventilation rate ($n=0.1 \text{ h}^{-1}$), contaminant concentration ϕ decreased exponentially and became 1/10 of the initial concentration level at 24 h from the beginning of the analysis.

Figure 4 shows the contaminant concentration ϕ distribution at 24 hours for two ventilation rates. Non-uniform concentration distributions were formed in the space. In the case of the low ventilation rate ($n=0.01 \text{ h}^{-1}$) in particular, the contaminant continuously stayed and accumulated at the center of the space and a high concentration zone was confirmed.

Figure 5 shows (S) and (I) distribution in the x - z plane at $y=1.6$ m height at 24 hours for three representative cases: Case 3, Case 7, and Case 11. In Case 3 as shown in Figure 5 (1) and (2), the distributions of (S) and (I) were similar, which was because (S) and (I) were assumed to be motionless and converted from (S) to (I) at the same points. (S) and (I) distributions indicated inhomogeneous distribution caused by non-uniform distribution of contaminant. In other words, there were inhomogeneous distributions of infection risk in the room. In Case 7, for which the diffusion of (S) and (I) was adopted, the distributions of (S) and (I) were spread throughout the entire space by movement. In Case 11, for which only the diffusion of (S) was analyzed, the distribution of (S) was almost the same as the result in Case 7. However, concerning (I), the distribution of (I) was similar to the result of Case 3, where the absolute value of (I) became large. This was because (S) moved to a high contaminant concentration region by diffusion and was converted to (I).

Figure 6 shows the time series of average values of (S) and (I) for each case. For Case 1 and Case 5, for which the ventilation rate was set to a relatively high level, namely, $n=0.1 \text{ h}^{-1}$, and the pulmonary ventilation rate was set to a low level, namely, $p=1.0 \times 10^{-5}$, β became almost zero in a short time scale and the time series of (S) and (I) showed constant values (the same as the initial values). In other cases, the time profile of (I) had a local maximum value and then decreased gradually. Considering the diffusion of (S) and (I), the number of (S) was decreased and that of (I) was increased compared with those for Case 1 - Case 4. In the

condition of Case 9 - Case 12 in which only (S) moved, time profiles of (S) and (I) were similar to those of Case 5 - Case 8, but the infection risk was estimated to be lower than that of Case 5 – Case 8, for which diffusions of both (S) and (I) were adopted.

Discussion

In this study, numerical analyses of unsteady and non-uniform concentration distribution by three-dimensional CFD and the procedures of coupled simulation between CFD and SIR-type epidemiological models were carried out. On the basis of these proposed procedures, the time dependence and distribution of infectious risk in indoor environments could be predicted quantitatively.

Contaminant concentration in the breathing zone was strongly influenced by the setting of the ventilation rate and therefore contact rate (β) was estimated as unsteady and inhomogeneous; then, space distributions of (S) and (I) were greatly changed in accordance with the boundary condition.

The scale of target spaces in this analysis was limited and grid scale was much smaller than the human scale. Analyses for larger spaces will be necessary in the future.

Furthermore, as shown in equations (1)-(3), constant (linear) and isotropic diffusion coefficients were adopted to reproduce movement of residents. In order to model human movement accurately, it is necessary to adopt a non-isotropic diffusion model and analysis by

cellular automata. This will also be investigated in the future.

Conclusion

In this study, the procedure of coupled analysis of unsteady and non-uniform concentration distribution based on CFD simulation and SIR-type epidemiology model was presented.

Furthermore, the results of sensitivity analysis related to the exposure risk assessment of aerial infectious contaminants were shown for large enclosed spaces.

The findings obtained from this study can be summarized as follows:

(1) The Wells-Riley equation, which was used for the oral exposure assessment and is a part of the classic SIR model by Kermack and McKendrick, indicated an initial infectious expansion period. In the assumption of a constant linear rate of pulmonary ventilation rate and contaminant concentration in the breathing zone, contact rate β can be directly estimated.

Through the analysis of infectious contaminant concentration level and non-uniform distribution in a large enclosure with CFD, the prediction of the number changes of (S), (I), and (R) becomes possible through the analysis of β .

(2) As a result of sensitivity analysis, the contaminant concentration in the breathing zone was found to be strongly dependent on the ventilation rate and then the distributions of (S) and (I) were greatly changed in accordance with initial and boundary conditions. We believe that the prediction procedures of coupled analysis of CFD and SIR model are effective for

infectious risk assessment in indoor environments with sufficient accuracy.

Acknowledgement

This research was partly supported by a Grant-in-Aid for Scientific Research (JSPS KAKENHI for Young Scientists (S), 21676005). The authors would like to express special thanks to the funding source.

References

- [1] Kermack, WO. and McKendrick, AG. (1927) A contribution to the mathematical theory of epidemics, *Proceedings of the Royal Society of London Series A*, **115**, 700-721
- [2] Wells, WF., (1955) Airborne contagion and air hygiene, Cambridge, MA, Harvard University Press
- [3] Riley, EC., Murphy, G. and Riley, RL. (1978) Airborne spread of measles in a suburban elementary school, *American Journal of Epidemiology*, **107**, 421-432
- [4] Li, Y., Huang, X., Yu, I.T.S., Wong, T.W., Qian, H. (2004) Role of air distribution in SARS transmission during the largest nosocomial outbreak in Hong Kong, *Indoor Air*, **15** (2) pp83-95
- [5] Hua Qian, et al., (2009) Spatial distribution of infection risk of SARS transmission in a hospital ward, *Building and Environment*, **44** (8), 1651-1658
- [6] Noakes, C.J., Beggs, C.B., Sleigh, P.A., and Kerr, K.G. (2006) Modeling the transmission of airborne infections in enclosed spaces, *Epidemiol. Infect.*, **134**, 1082-1091
- [7] Fine, P.E.M., (1993) Herd immunity: history, theory, practice, *Epidemiological Review* **15** (2): 265-302

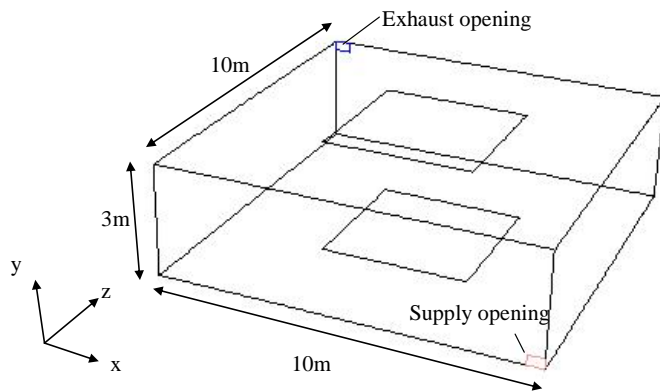


Figure 1 Outline of target spaces

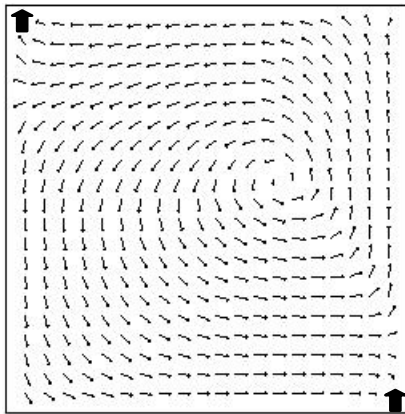


Figure 2 Results of flow field ($n=0.01 \text{ h}^{-1}$, $y=1.6 \text{ m}$ height, x - z plane)

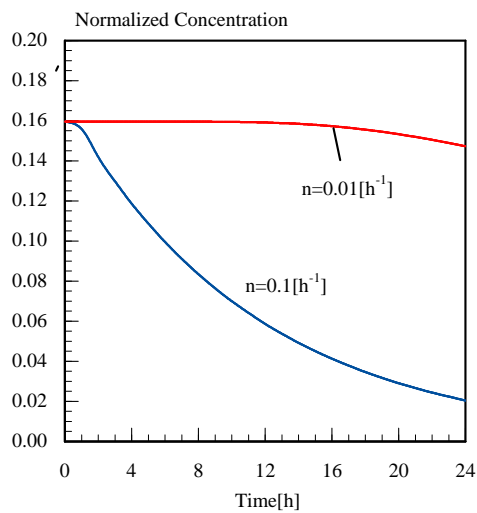
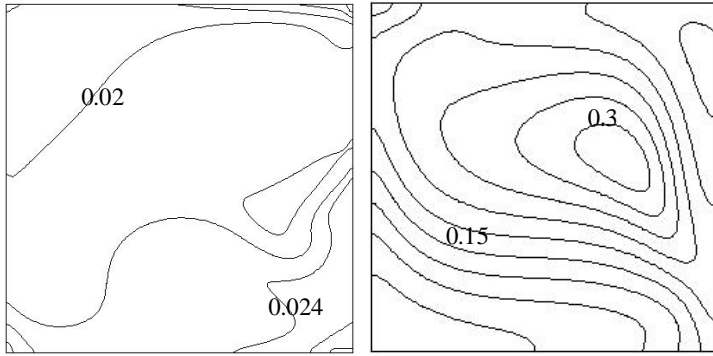


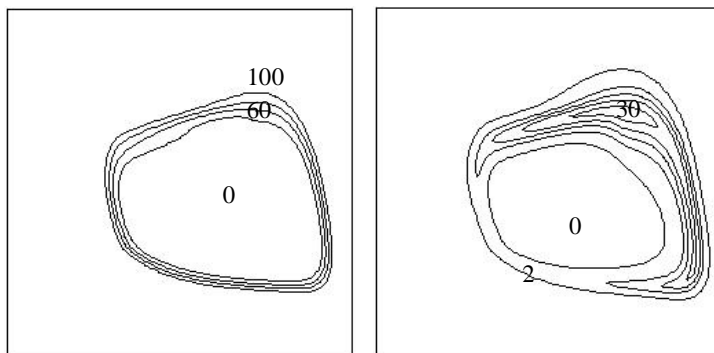
Figure 3 Time series of contaminant concentration ϕ for two ventilation rates (volume-averaged concentration, $y=1.6 \text{ m}$, x - z plane)



(1) $\phi (n=0.1 \text{ h}^{-1})$

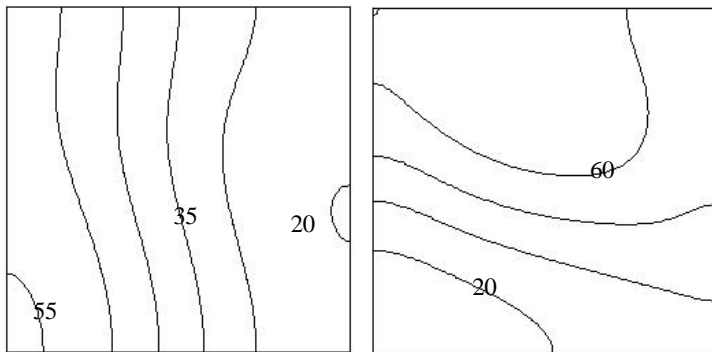
(2) $\phi (n=0.01 \text{ h}^{-1})$

Figure 4 Normalized concentration distribution ($t=24 \text{ h}$, $y=1.6 \text{ m}$, $x\text{-}z$ plane)



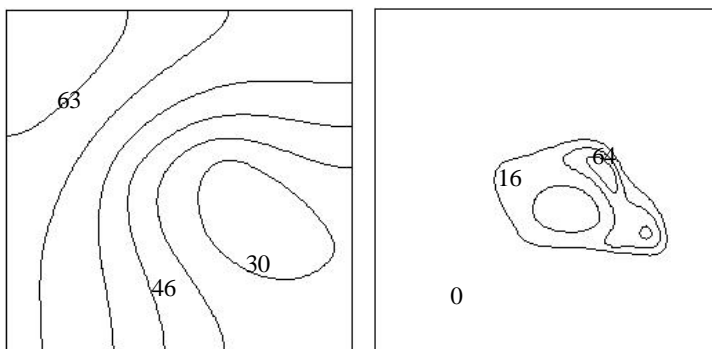
(1) S (Case 3)

(2) I (Case 3)



(3) S (Case 7)

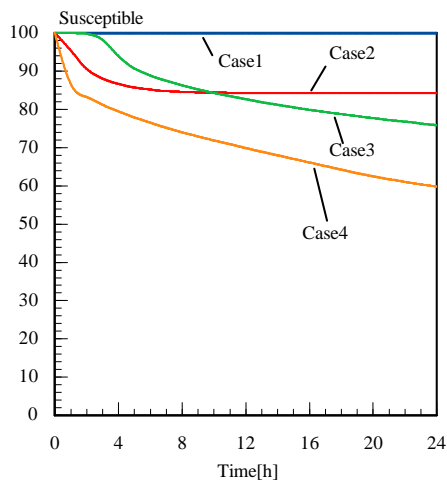
(4) I (Case 7)



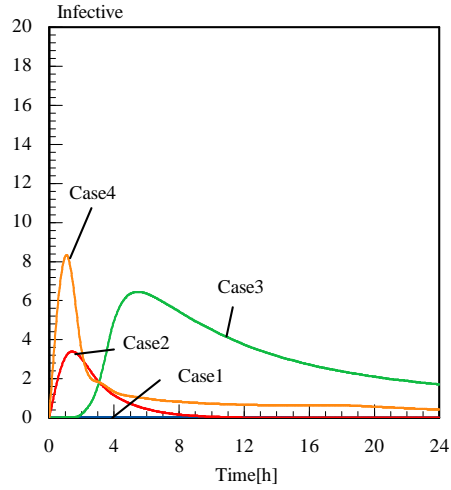
(5) S (Case 11)

(6) I (Case 11)

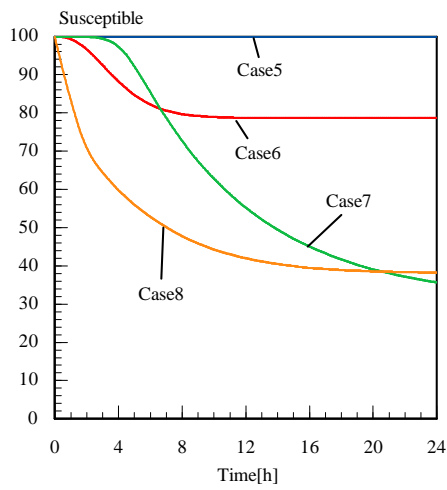
Figure 5 Population density distributions of (S) and (I) ($y=1.6 \text{ m}$, $t=24 \text{ h}$, $x\text{-}z$ plane)



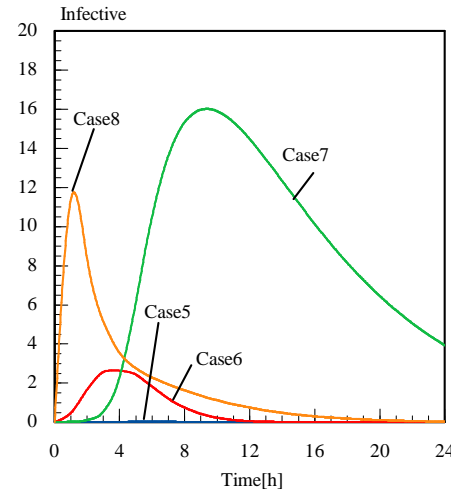
(1) S (Cases 1 - 4)



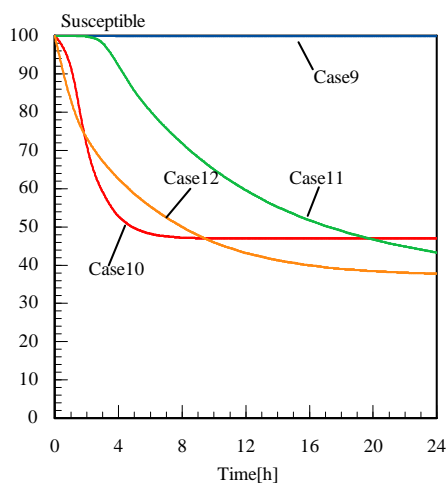
(5) I (Cases 1 - 4)



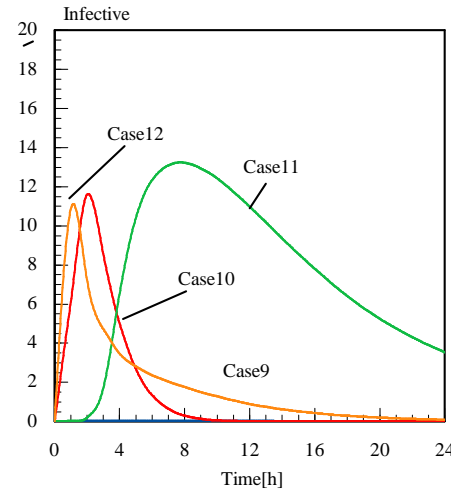
(2) S (Cases 5 - 8)



(6) I (Cases 5 - 8)



(3) S (Cases 9 - 12)



(7) I (Cases 9 - 12)

Figure 6 Time series of population density of (S) and (I) for each case

Table 1 SIR Model and Wells-Riley Model

[1] SIR (Kermack and McKendrick) model	
$\frac{dS}{dt} = -\beta SI + \nabla(D_S \nabla S), \quad \beta = p\phi$	(1)
$\frac{dI}{dt} = -\gamma I + \beta SI + \nabla(D_I \nabla I)$	(2)
$\frac{dR}{dt} = \gamma I + \nabla(D_R \nabla R)$	(3)
$R_o = \frac{\beta}{\gamma} S_o$	(4)
[2] Scalar transport equation	
$\frac{\partial \phi}{\partial t} + \nabla \phi \mathbf{u} = \nabla(D \nabla \phi) + S_\phi$	(5)
[3] Wells-Riley model	
$P_I = \frac{C}{S} = 1 - \exp\left(-\frac{Iqpt}{Q}\right)$	(6)
[4] Relations between each constant of Wells-Riley and SIR	
$S = S_o \exp(-\beta It)$	(7)
$I = S_o - S \exp(-\beta It)$	(8)
$P_I = \frac{I}{S_o} = 1 - \exp(-\beta It)$	(9)
$\beta = \frac{qp}{Q}$	(10)

Table 2 Numerical and Boundary Conditions

Turbulence Model	RNG k-ε model (3-dimensional Cal.)
Scheme	Convection Term: QUICK
Inflow Boundary	$U_{in} = 0.07$ [m/s] for $n = 0.1$ [h ⁻¹], $U_{in} = 0.007$ [m/s] for $n = 0.01$ [h ⁻¹], $k_{in} = 3/2 \times (U_{in} \times 0.1)^2$, $\varepsilon_{in} = \mu^{3/4} \times k_{in}^{3/2} / l_{in}$, $C_\mu = 0.09$, $l_{in} = 0.044$ [m]
Outflow Boundary	$U_{out} =$ free slip, $k_{out} =$ free slip, $\varepsilon_{out} =$ free slip
Wall Treatment	Velocity; generalized log low
Contaminant	Passive Contaminant
SIR Model	$S_o = 100$, $I_o = 10^{-2}$, $R_o = 10$

Table 3 Cases analyzed

Case	Ventilation Rate n [h ⁻¹]	Pulmonary Ventilation Rate p [m ³ /s]	Diffusion Coefficient	
			D_S [m ² /s]	D_I [m ² /s]
Case 1	0.1	1.0×10^{-5}	0	0
Case 2	0.1	5.0×10^{-5}	0	0
Case 3	0.01	1.0×10^{-5}	0	0
Case 4	0.01	5.0×10^{-5}	0	0
Case 5	0.1	1.0×10^{-5}	2.8×10^{-3}	2.8×10^{-3}
Case 6	0.1	5.0×10^{-5}	2.8×10^{-3}	2.8×10^{-3}
Case 7	0.01	1.0×10^{-5}	2.8×10^{-4}	2.8×10^{-4}
Case 8	0.01	5.0×10^{-5}	2.8×10^{-4}	2.8×10^{-4}
Case 9	0.1	1.0×10^{-5}	2.8×10^{-3}	0
Case 10	0.1	5.0×10^{-5}	2.8×10^{-3}	0
Case 11	0.01	1.0×10^{-5}	2.8×10^{-4}	0
Case 12	0.01	5.0×10^{-5}	2.8×10^{-4}	0